

Unconditional Steady-State Entanglement in Macroscopic Hybrid Systems by Coherent Noise Cancellation

Xinyao Huang,^{1,2} Emil Zeuthen,^{2,*} Denis V. Vasilyev,^{3,4} Qiongyi He,^{1,†} Klemens Hammerer,⁵ and Eugene S. Polzik²

¹*State Key Laboratory of Mesoscopic Physics, School of Physics, Peking University, Collaborative Innovation Center of Quantum Matter, Beijing 100871, China*

²*Niels Bohr Institute, University of Copenhagen, DK-2100 Copenhagen, Denmark*

³*Center for Quantum Physics, Faculty of Mathematics, Computer Science and Physics, University of Innsbruck, A-6020 Innsbruck, Austria*

⁴*Institute for Quantum Optics and Quantum Information of the Austrian Academy of Sciences, A-6020 Innsbruck, Austria*

⁵*Institute for Theoretical Physics and Institute for Gravitational Physics (Albert Einstein Institute), Leibniz Universität Hannover, Callinstr. 38, 30167 Hannover, Germany*



(Received 8 January 2018; published 5 September 2018)

The generation of entanglement between disparate physical objects is a key ingredient in the field of quantum technologies, since they can have different functionalities in a quantum network. Here we propose and analyze a generic approach to steady-state entanglement generation between two oscillators with different temperatures and decoherence properties coupled in cascade to a common unidirectional light field. The scheme is based on a combination of coherent noise cancellation and dynamical cooling techniques for two oscillators with effective masses of opposite signs, such as quasispin and motional degrees of freedom, respectively. The interference effect provided by the cascaded setup can be tuned to implement additional noise cancellation leading to improved entanglement even in the presence of a hot thermal environment. The unconditional entanglement generation is advantageous since it provides a ready-to-use quantum resource. Remarkably, by comparing to the conditional entanglement achievable in the dynamically stable regime, we find our unconditional scheme to deliver a virtually identical performance when operated optimally.

DOI: [10.1103/PhysRevLett.121.103602](https://doi.org/10.1103/PhysRevLett.121.103602)

Entanglement is a peculiar property of quantum physics and a key technological resource in quantum information processing [1] and quantum metrology [2,3], allowing improvements of atomic clocks [4,5] and optical magnetometers [6,7]. Moreover, entanglement is often used to delineate the boundary between classical and quantum physics. Generating entanglement for ever-larger objects therefore establishes the reach of quantum mechanics into the macroscopic realm. Entanglement between separate macroscopic systems has already been realized with pairs of atomic vapor ensembles [7–9] and diamonds [10] at room temperature, and mechanical oscillators at cryogenic temperatures [11,12]. However, generation of entanglement in hybrid systems composed of disparate macroscopic objects is an outstanding challenge—in particular due to the presence of the hot thermal environment. Such hybrid entanglement would combine attractive features of very different systems as required to realize complex quantum information networks [13].

In this Letter, we devise an efficient scheme for unconditionally entangling two macroscopic systems with potentially very different decoherence properties. The scheme works for two generic bosonic oscillators coupled linearly to a unidirectional traveling light field, with the extra

provision that their effective masses have opposite signs. A negative mass oscillator in the entanglement context was first used in Ref. [8], and further extensively developed for collective degrees of freedom in polarized spin ensembles prepared in an energetically inverted state [14,15] such as in atomic ensembles at room temperature in free space [16,17], cold atoms in Bose-Einstein condensates [18], optical cavities [19,20], or trapped in one-dimensional arrays [21,22] as well as in solid-state ensembles of nitrogen-vacancy centers [23] and quasispins of rare-earth-ion doped crystals [24,25]. The positive mass subsystem can, naturally, be implemented in a wider range of systems, in particular in motional degrees of freedom, e.g., the center-of-mass motion of ensembles of atoms [20,26,27] or ions [28] and micromechanical oscillators [11,12,29–31]. A motional degree of freedom can also implement an effective negative mass by employing two-tone driving schemes [32] (see also Ref. [33]).

An essential mechanism of our scheme is coherent quantum noise cancellation (CQNC) of the backaction (BA) of light on the two oscillators. This hinges on the observation that for two oscillators with masses of opposite signs, $m_+ = -m_- := m > 0$, we have $(d/dt)[\hat{X}_+ + \hat{X}_-] = [\hat{P}_+ - \hat{P}_-]/m$ for which $[\hat{X}_+ + \hat{X}_-, \hat{P}_+ - \hat{P}_-] = 0$, where

\hat{X}_\pm and \hat{P}_\pm are canonical conjugate variables for the positive (negative) mass oscillator. Hence, this pair of variables is classical in the sense that the Heisenberg uncertainty relation imposes no constraint on the simultaneous knowledge of them [8,14,15]. This is possible because (for ideally matched oscillators) the associated measurement BA goes into the canonically conjugate joint variables, while interfering destructively in the BA-free variables. Measuring the latter beyond the Heisenberg limit of the individual systems entails entanglement between the two oscillators. CQNC based on this principle has previously been analyzed theoretically in the context of sensing beyond the standard quantum limit (SQL) [14,34–38] and realized experimentally using two mechanical oscillators [32] and in a spin-optomechanical hybrid system [39]. It has also been analyzed as a means of entangling two atomic spin [40,41] or mechanical [35,42] systems as has been demonstrated in experiment [7–9,12].

However, the theoretical studies have mostly focused on oscillators with identical or negligible intrinsic linewidths, a condition which is difficult to meet in practice for disparate hybrid systems. The present scheme circumvents this restriction by interfacing the two oscillators unidirectionally. The resulting causal asymmetry permits efficient CQNC even for vastly different intrinsic linewidths, thereby facilitating entanglement generation.

Model.—We consider a generic hybrid system composed of two subsystems with effective masses $\text{sgn}(m_S) = -\text{sgn}(m_M) < 0$ coupled to a unidirectional optical field [Fig. 1] (near-ideal unidirectionality has been achieved experimentally, e.g., see Refs. [7,39]). Both subsystems are driven by individual thermal reservoirs. The positive (negative) mass subsystem is referred to as a motional [M] (collective spin [S]) degree of freedom and represented by a localized bosonic mode with dimensionless canonical variables. These variables satisfy $[\hat{X}_j, \hat{P}_k] = i\delta_{j,k}$, ($j, k \in \{M, S\}$) resulting from a rescaling by the zero-point fluctuation amplitudes $x_{j,\text{zpf}} = \sqrt{\hbar/(|m_j|\omega_j)}$ and $p_{j,\text{zpf}} = \hbar/x_{j,\text{zpf}}$, where ω_j is the resonance frequency. The free evolution of the hybrid system is (setting $\hbar = 1$)

$$\hat{H}_0 = \sum_{j \in \{M, S\}} \text{sgn}(m_j) \frac{\omega_j}{2} (\hat{X}_j^2 + \hat{P}_j^2), \quad (1)$$

and hence a negative mass translates into a negative effective resonance frequency $\Omega_j \equiv \text{sgn}(m_j)\omega_j$ for the dimensionless variables, inverting the sense of rotation in the $\{\hat{X}_j, \hat{P}_j\}$ phase space (Fig. 1) and making the state with zero quanta its *highest* energy state (not to be confused with a positive mass oscillator with an inverted potential, $\hat{H}_0 \propto -\hat{X}_j^2 + \hat{P}_j^2$). We specialize to the resonant scenario $\omega_M = \omega_S := \omega$.

We introduce annihilation operators for the localized modes, $\hat{X}_j = (\hat{a}_j + \hat{a}_j^\dagger)/\sqrt{2}$ and $\hat{P}_j = (\hat{a}_j - \hat{a}_j^\dagger)/(\sqrt{2}i)$,

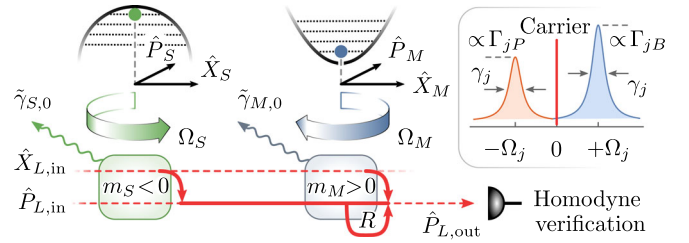


FIG. 1. Hybrid system consisting of two oscillators with negative and positive mass, respectively, typically implemented in collective spin (S) and motional (M) degrees of freedom. These are coupled in cascade to a common unidirectional light field via quadratic interactions induced typically by a strong, classical carrier. For each oscillator, this results in Stokes and anti-Stokes sidebands proportional to rates $\Gamma_{jP/B}$ and of width γ_j , $j \in \{S, M\}$ (see inset); the effective resonance frequency $\Omega_j \equiv \text{sgn}(m_j)\omega_j$ accounts for, e.g., the fact that energy must be extracted from a negative-mass oscillator to excite it. The joint interaction with the light field is best described by homodyne quadratures \hat{X}_L, \hat{P}_L (symmetrized combinations of sidebands), whose initial state $\hat{X}_{L,\text{in}}, \hat{P}_{L,\text{in}}$ is vacuum (see lower part of figure). The negative mass system is driven by $\hat{X}_{L,\text{in}}$ only ($\Gamma_{SP} = \Gamma_{SB}$) and its response is mapped onto \hat{P}_L . The positive mass system is likewise coupled to $\hat{X}_{L,\text{in}}$, but also to \hat{P}_L ($\Gamma_{MP} < \Gamma_{MB}$) at an adjustable rate R , so that the response of the negative mass system drives the positive mass system. Consequently, the response of the positive mass system will interfere destructively with that of the negative mass system in the outgoing field quadrature $\hat{P}_{L,\text{out}}$ as can (optionally) be verified by homodyne detection. Additionally, the oscillators are driven by distinct thermal reservoirs with decoherence rates $\tilde{\gamma}_{j,0}$ (wavy arrows).

and the propagating field linking them, $\hat{b}(t) = (2\pi)^{-1/2} \int_{-\infty}^{\infty} \hat{b}(\Omega) e^{-i\Omega t} d\Omega$ (defined in a rotating frame with respect to the optical carrier). The Hamiltonian for two-mode quadratic interaction between the localized oscillators and the light field is [40,41]

$$\hat{H}_{\text{int}} = \sum_{j \in \{M, S\}} [\sqrt{\Gamma_{jB}} \hat{a}_j^\dagger \hat{b}(t_j) + \sqrt{\Gamma_{jP}} \hat{a}_j^\dagger \hat{b}^\dagger(t_j) + \text{H.c.}], \quad (2)$$

where we assume $t_S < t_M$; i.e., the optical field interacts with S first. Equation (2) comprises two kinds of interaction: beam splitter (B), $\propto (\hat{a}_j^\dagger \hat{b} + \text{H.c.})$, and parametric down-conversion (P), $\propto (\hat{a}_j^\dagger \hat{b}^\dagger + \text{H.c.})$, $j \in \{M, S\}$. These processes produce sidebands at rates $\Gamma_{jB} = \Gamma_j \sin^2 \theta_j$, $\Gamma_{jP} = \Gamma_j \cos^2 \theta_j$ (Fig. 1, inset), which we parametrize by $\Gamma_j = \Gamma_{jB} + \Gamma_{jP}$ and $\theta_j \in [0, \pi/2]$, the coupling rates and angles.

An excitation in the upper sideband from the positive-(negative-)mass oscillator arises from $\sqrt{\Gamma_{MB}} \hat{a}_M \hat{b}^\dagger$ ($\sqrt{\Gamma_{SP}} \hat{a}_S \hat{b}^\dagger$), simultaneously removing (adding) an oscillator quantum (analogously for the lower sideband).

This indistinguishability of adding a quantum to one subsystem and removing one from the other as energy is either added or removed by the common light field permits the system to be driven into a two-mode-squeezed entangled state accompanied by CQNC of the BA contribution to the joint output field. Perfect indistinguishability necessitates $\Gamma_{MB} = \Gamma_{SP}$ and $\Gamma_{MP} = \Gamma_{SB}$, i.e., $\theta_M = -\theta_S + \pi/2$ and $\Gamma_M = \Gamma_S$, but also the temporal responses of the subsystems must be suitably matched. However, whenever $\theta_M \neq \theta_S$ there is an overlap between the light quadrature reading out S and the quadrature driving M ; i.e., the spin response to light and thermal forces drives the motional mode. This induces a tunable interference effect that can implement additional quantum and classical noise cancellation even for highly asymmetric subsystems, leading to unconditional entanglement generation competitive with conditional schemes—this is the main finding of this Letter.

The regime of interest is $\omega_j \gg \Gamma_j \gtrsim \tilde{\gamma}_{j,0}$, where $\tilde{\gamma}_{j,0}$ is the thermal decoherence rate, providing the time-scale separation required for probing the system over several quantum-coherent oscillations. This permits treating Eq. (2) in the rotating wave approximation (RWA), i.e., retaining only slowly varying terms, and implies that the interaction with light is confined to two disjoint sidebands $\hat{b}_-(t) + \hat{b}_+(t) := (2\pi)^{-1/2}(\int_{-\infty}^0 + \int_0^{\infty})\hat{b}(\Omega)e^{-i\Omega t}d\Omega = \hat{b}(t)$, $[\hat{b}_{\pm}(t), \hat{b}_{\pm}^{\dagger}(t')] = \delta(t-t')$, centered at frequencies $\Omega = \mp \omega$ (relative to the carrier). We introduce the non-Hermitian homodyne two-mode quadratures $\hat{X}_L := (\hat{b}_+ + \hat{b}_-^{\dagger})/\sqrt{2}$ and $\hat{P}_L := (\hat{b}_+ - \hat{b}_-^{\dagger})/(\sqrt{2}i)$. Performing the RWA we find

$$\hat{H}_{\text{int}} \approx \hat{a}_M^{\dagger} \sqrt{\Gamma_M} \hat{Q}_{\theta'_M}(t_M) + \hat{a}_S \sqrt{\Gamma_S} \hat{Q}_{-\theta'_S}(t_S) + \text{H.c.}, \quad (3)$$

where $\hat{Q}_{\theta'} := \cos \theta' \hat{X}_L + i \sin \theta' \hat{P}_L$, $\theta'_j = \theta_j - \pi/4$. Equation (3) indicates that the cosine and sine components of the phase quadrature $\propto \hat{P}_L + \hat{P}_L^{\dagger}$ read out the (unnormalized) EPR-type variables $\sqrt{\Gamma_M} \cos \theta'_M \hat{X}_M + \sqrt{\Gamma_S} \cos \theta'_S \hat{X}_S$ and $\sqrt{\Gamma_M} \cos \theta'_M \hat{P}_M - \sqrt{\Gamma_S} \cos \theta'_S \hat{P}_S$, respectively. These commute when $\sqrt{\Gamma_M} \cos \theta'_M = \sqrt{\Gamma_S} \cos \theta'_S$, in which case they can be BA-free.

Eliminating the light field and using a co-propagating time coordinate $t' = t - x/c$ (dropping the prime henceforth), the Heisenberg-Langevin equations can be expressed in terms of the forces $\hat{f}_j := \sqrt{\gamma_{j,0}} \hat{a}_{j,\text{in}} + \hat{f}_{j,\text{BA}}$ as [henceforth \hat{a}_j is in the rotating frame of \hat{H}_0 (1)] [43–45]

$$\begin{aligned} \frac{d}{dt} \hat{a}_S &= -\frac{\gamma_S}{2} \hat{a}_S + \hat{f}_S, \\ \frac{d}{dt} \hat{a}_M &= -\frac{\gamma_M}{2} \hat{a}_M + \hat{f}_M + \sqrt{1 - \epsilon R} \hat{a}_S^{\dagger}, \end{aligned} \quad (4)$$

where

$$\begin{aligned} \hat{f}_{S,\text{BA}} &:= -i(\sqrt{\Gamma_{SB}} \hat{b}_{-, \text{in}} + \sqrt{\Gamma_{SP}} \hat{b}_{+, \text{in}}^{\dagger}), \\ \hat{f}_{M,\text{BA}} &:= -i\sqrt{1 - \epsilon}(\sqrt{\Gamma_{MB}} \hat{b}_{+, \text{in}} + \sqrt{\Gamma_{MP}} \hat{b}_{-, \text{in}}^{\dagger}) \\ &\quad - i\sqrt{\epsilon}(\sqrt{\Gamma_{MB}} \hat{b}_{+, \text{in}}' + \sqrt{\Gamma_{MP}} \hat{b}_{-, \text{in}}'^{\dagger}). \end{aligned} \quad (5)$$

Here, an additional uncorrelated vacuum $\hat{b}'_{\pm, \text{in}}$ impinges on M due to transmission (power) loss $\epsilon > 0$ between the subsystems. The vacuum fields satisfy $\langle \hat{b}_{\pm, \text{in}}(t) \hat{b}_{\pm, \text{in}}^{\dagger}(t') \rangle = \langle \hat{b}'_{\pm, \text{in}}(t) \hat{b}'_{\pm, \text{in}}{}^{\dagger}(t') \rangle = \delta(t-t')$. $[\hat{a}_{j,\text{in}}(t), \hat{a}_{j,\text{in}}^{\dagger}(t')] = \delta(t-t')$, $j \in \{M, S\}$, represent the thermal noise fluctuations with $\langle \hat{a}_{j,\text{in}}(t) \hat{a}_{j,\text{in}}^{\dagger}(t') \rangle = (\bar{n}_j + 1)\delta(t-t')$ in terms of the thermal occupancy \bar{n}_j . For example, for S , $\bar{n}_S > 0$ represents the additional noise present for an imperfectly polarized ensemble, while for M , $\bar{n}_M \approx k_B T_M / (\hbar \omega_M)$ at ambient temperature T_M (k_B is the Boltzmann constant). The effective linewidths (including dynamical broadening from the light field coupling) are denoted $\gamma_j = \gamma_{j,0} - \Gamma_j \cos(2\theta_j)$, where $\gamma_{j,0}$ is the linewidth in absence of dynamical broadening; dynamical stability requires $\gamma_j > 0$. Finally, due to the unidirectionality of the light field, information can only propagate from the first to the second subsystem in the cascade. The corresponding unidirectional coupling rate is $R = \sqrt{\Gamma_{SB}} \Gamma_{MP} - \sqrt{\Gamma_{MB}} \Gamma_{SP} = -\sqrt{\Gamma_M \Gamma_S} \sin(\theta_M - \theta_S)$. For $R = 0 \Leftrightarrow \theta_S = \theta_M$, Eqs. (4) decouple so that correlations build up solely due to those between $\hat{f}_{S,\text{BA}}$ and $\hat{f}_{M,\text{BA}}$, and the ordering of oscillators becomes immaterial (assuming $\epsilon = 0$). In contrast, $R \neq 0$ gives rise to a nontrivial asymmetry of the cascaded system (4), which is exploited below for improved noise cancellation and entanglement generation.

Unconditional steady-state solution.—The steady-state solution to Eqs. (4) is

$$\begin{aligned} \hat{a}_S(t) &= \int_{-\infty}^t dt' e^{-(t-t')\gamma_S/2} \hat{f}_S(t'), \\ \hat{a}_M(t) &= \int_{-\infty}^t dt' \{ e^{-(t-t')\gamma_M/2} \hat{f}_M(t') \\ &\quad + \frac{2\sqrt{1 - \epsilon R}}{\gamma_M - \gamma_S} [e^{-(t-t')\gamma_S/2} - e^{-(t-t')\gamma_M/2}] \hat{f}_S^{\dagger}(t') \}. \end{aligned} \quad (6)$$

For $R = 0$, the steady states of the individual subsystems are determined solely by the (stochastic) driving forces in the past time interval of duration $\sim 1/\gamma_j$. Hence, whenever $\gamma_M \neq \gamma_S$ the different temporal responses to the BA $\hat{b}_{\pm, \text{in}}$ will result in imperfect CQNC. However, if it is the second system (M) in the cascade which is relatively short-lived, $\gamma_M > \gamma_S$, then for $R \neq 0$ the unidirectional coupling term $\propto R \hat{a}_S^{\dagger}$ [Eq. (4)] effectively prolongs the memory time $1/\gamma_M$ by driving M with the spin response contained in the light field, resulting in improved CQNC for $R < 0 \Leftrightarrow \theta_M > \theta_S$. Ideal cancellation can be achieved in the adiabatic limit $\gamma_M \gg \gamma_S$ and $2R/\gamma_M \rightarrow -1$ (for $\epsilon = 0$) [Eq. (6)], which is compatible with the demand for near-ground-state dynamical cooling of the motional mode $\gamma_M \gg \tilde{\gamma}_{M,0}$, where

$\tilde{\gamma}_{j,0} := \gamma_{j,0}(\bar{n}_j + 1/2)$. The additional interference arising for $R < 0$ does not rely on the opposite signs of masses (in contrast to the scheme as a whole) and can simultaneously suppress both quantum noise and the spin thermal noise, thereby removing the need for dynamical spin cooling.

From Eqs. (6) the entries of the covariance matrix in steady state are

$$\begin{aligned} \Delta^2 \hat{X}_S &= \frac{1}{\gamma_S} \left(\frac{\Gamma_S}{2} + \tilde{\gamma}_{S,0} \right), \\ \Delta^2 \hat{X}_M &= \frac{1}{\gamma_M} \left(\frac{\Gamma_M}{2} + \tilde{\gamma}_{M,0} + \sqrt{1 - \epsilon R} \langle \hat{X}_S, \hat{X}_M \rangle \right), \\ \langle \hat{X}_S, \hat{X}_M \rangle &= -\frac{2\sqrt{1 - \epsilon}}{\gamma_S + \gamma_M} \left(\sqrt{\Gamma_S \Gamma_M} \sin(\theta_M + \theta_S) - 2R \Delta^2 \hat{X}_S \right), \end{aligned} \quad (7)$$

where $\langle \hat{X}_S, \hat{X}_M \rangle := \langle \hat{X}_S \hat{X}_M \rangle + \langle \hat{X}_M \hat{X}_S \rangle - 2\langle \hat{X}_S \rangle \langle \hat{X}_M \rangle$. As our entanglement figure of merit we consider the variance of generalized EPR variables of the form [46,47]

$$\xi_g = \frac{\Delta^2(\hat{X}_S + g\hat{X}_M) + \Delta^2(\hat{P}_S - g\hat{P}_M)}{1 + g^2} < 1, \quad (8)$$

which is the inseparability criterion for Gaussian states and any $g \in \mathbb{R}$. The steady-state value of ξ_g can be evaluated using the solution (7), noting that $\Delta^2(\hat{X}_S + g\hat{X}_M) \approx \Delta^2(\hat{P}_S - g\hat{P}_M)$ within the RWA. In principle, ξ_g can be minimized over g , but verifying such entanglement experimentally requires individual, and hence destructive, readout of the two subsystems. Since our scheme automatically and nondestructively produces readout of the EPR variables with $g = \sqrt{\Gamma_M / [(1 - \epsilon)\Gamma_S]} \cos \theta'_M / \cos \theta'_S$ [see discussion below Eq. (3)], which can be BA-free when $g \rightarrow 1$ and $\epsilon \rightarrow 0$, we henceforth fix g by the aforementioned expression.

Spin-optomechanical implementation.—Let us consider a spin-optomechanical implementation [16,48] [see Ref. [49] for a derivation of Eqs. (4), (5) in this context]. Optomechanical systems are routinely operated in the quantum regime, allowing ground-state cooling by dynamical broadening ($\gamma_M > \gamma_{M,0} \Leftrightarrow \theta_M > \pi/4$) even for $\bar{n}_M \gg 1$. For the mechanical system, $\gamma_{M,0}$ is usually due to intrinsic dissipation alone, such as friction, whereas for the spin oscillator, $\gamma_{S,0}$ (typically $\gg \gamma_{M,0}$) is often dominated by optical power broadening induced by the coherent driving. For quantum cooperativities defined as $C_j := \Gamma_j / \tilde{\gamma}_{j,0}$, the value of C_S is independent of the drive power in this regime.

Conditional entanglement in a spin-optomechanical system was previously analyzed for a pulsed quantum non-demolition (QND) measurement of the hybrid EPR variables [57] which projects the system into an entangled state fulfilling Eq. (8); this approach has been demonstrated for two atomic spin ensembles [8]. In contrast to that protocol, steady-state unconditional entanglement is a ready-to-use resource [9,58] available on demand at any moment in time.

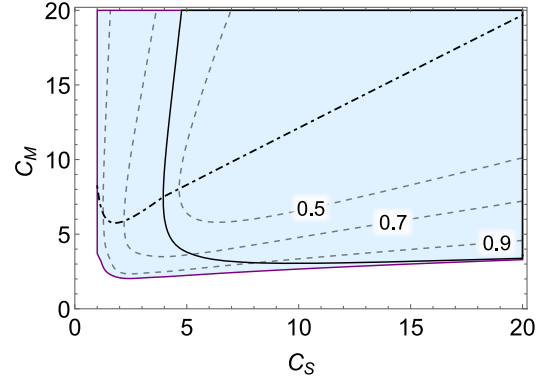


FIG. 2. Entanglement ξ_g (< 1 in the colored region) as a function of quantum cooperativities of the spin (C_S) and motional (C_M) subsystems for optimized coupling angles θ_S and θ_M while fixing the parameters $\gamma_{S,0} = 2\pi \times 5$ kHz, $\bar{n}_S = 1$, $\gamma_{M,0}\bar{n}_M = 2\pi \times 10$ kHz, and assuming no transmission losses, $\epsilon = 0$. Optimal C_M for given C_S is indicated by the dashed-dotted curve. Imposing the additional constraint $\theta_S = \theta_M \Rightarrow R = 0$, entanglement $\xi_g < 1$ is only possible in the subregion delineated by the solid contour.

Figure 2 presents the optimized unconditional steady-state entanglement (8) as a function of C_j , illustrating the relaxation of parameter requirements compared to dissipative entanglement generation ($R = 0$, both subsystems are driven optically only by the common vacuum field). Since the tunability of free-space spin systems is limited by the atomic density, we henceforth assume the bottleneck to be the spin system, characterized by a maximally attainable C_S , whereas C_M is freely tunable and thus can be fixed at its optimal value [Fig. 2, dashed-dotted curve]. Under these conditions, optimization requires the two subsystems to be coupled asymmetrically to the field: The optimal θ_M favors beam-splitter interaction $\pi/2 \geq \theta_{M,\text{opt}} > \pi/4$, while for S , the Stokes and anti-Stokes processes should be balanced, $\theta_{S,\text{opt}} \approx \pi/4 \Leftrightarrow \Gamma_{SB} \approx \Gamma_{SP}$ (QND interaction) yielding $R < 0$ [Fig. 3, inset]; this is the scenario illustrated in Fig. 1. The resulting effective motional linewidth considerably exceeds that of S , $\gamma_M \gg \gamma_S$, in the regime of substantial entanglement, thereby reversing the hierarchy set by the intrinsic linewidths $\gamma_{M,0} \ll \gamma_{S,0}$ while providing strong dynamical cooling of the motional thermal noise $\tilde{\gamma}_{M,0}$, which is essential to unconditional operation. Since $\gamma_S \sim \gamma_{S,0}$ for $\theta_S \approx \pi/4$, the suppression of spin thermal noise is due mainly to coherent cancellation in contrast to previous work relying on dynamical spin cooling in the dissipative regime ($R \approx 0$) [9,40,41].

In the absence of transmission loss ($\epsilon = 0$), the asymptotic scaling of the unconditional entanglement is $\xi_g \approx \sqrt{[1 + r + 1/(2\bar{n}_S + 1)]/(2C_S)}$, where $r = \tilde{\gamma}_{M,0}/\tilde{\gamma}_{S,0}$. An improvement by up to a factor of 2 can be found when comparing to the dissipative case ($R = 0$), $\xi_g \approx \sqrt{2(1 + r)/C_S}$ (see Fig. 3; derivations of scalings are in Ref. [49]). The presence of loss $\epsilon > 0$ imposes a lower

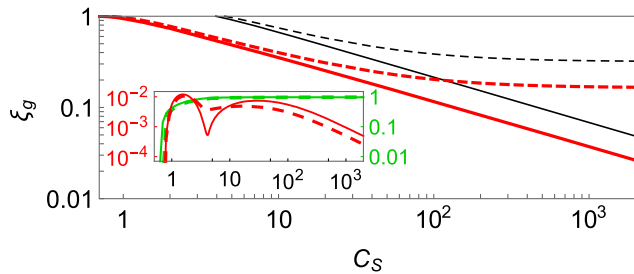


FIG. 3. Entanglement ξ_g as a function of spin cooperativity C_S for optimized coupling angles θ_S, θ_M and motional cooperativity C_M when $R = 0$ (thin black curves) and $R \neq 0$ (thick red curves), when transmission loss is absent, $\epsilon = 0$ (solid), and present, $\epsilon = 0.1$ (dashed). (Inset) Plot of $-2\sqrt{1-\epsilon R}/\gamma_M$ (right scale, brighter green curves) as a function of C_S used in evaluating the optimized curves of the main plot, and the relative entanglement improvement (left scale, darker red curves) of the conditional scheme over the optimal unconditional scheme (referenced to the latter) for $\epsilon = 0.1$; the conditional performance is evaluated using parameters optimized for the unconditional scheme (dashed) and optimal conditional parameters for QND readout $\theta_S = \theta_M = \pi/4$ (solid). The fixed parameters are $\gamma_{S,0} = 2\pi \times 5$ kHz, $\bar{n}_S = 1$, and $\gamma_{M,0}\bar{n}_M = 2\pi \times 10$ kHz.

bound $\xi_g \geq \sqrt{\epsilon/(4-3\epsilon)}$, which is also an improvement of up to a factor of 2 compared to $R = 0$.

Comparison with conditional scheme.—Another benchmark is the conditional steady-state entanglement generated by performing a continuous homodyne measurement of the light field emanating from the hybrid system [41]. The evolution of the system conditioned on the measurement record is described by a stochastic master equation [59] whose steady state can be found numerically and even analytically in our regime of interest, $\bar{n}_M \gg 1$ (see Ref. [49] for mathematical details). For the fixed parameters considered above (Fig. 3), we find in the limit of substantial entanglement that, remarkably, the conditional steady-state entanglement matches that of our unconditional scheme within a few-percent margin, even when separately optimized under the same conditions in the dynamically stable regime (see Fig. 3, inset; supplementary details in Ref. [49]). We thus conclude that our unconditional scheme leaves practically no information in the output light about the noise affecting the squeezed EPR variables. From a practical standpoint this is beneficial as it allows optimal performance without the need to measure the output field nor perform the feedback required to make the conditional entanglement unconditional. Moreover, the dynamical cooling of the motional mode occurring in the unconditional scheme facilitates technical stability in the apparatus.

In conclusion, unconditional steady-state entanglement in a cascaded negative-positive mass hybrid system can be efficiently generated by engineering an asymmetric interaction between the subsystems via the light field connecting them. Applications for such a resource of ready-to-use entanglement include quantum teleportation [60] and key

distribution [61] in hybrid quantum networks. The scheme can compete with conditional schemes, a fact which we speculate can be elucidated by formally framing our unconditional scheme in terms of a coherent-feedback master equation. The noise cancellation technique inherent to the scheme enables sub-SQL sensitivity when using the hybrid system as a continuous force sensor, as will be elaborated on elsewhere [62]. Moreover, we have evidence that this sensing enhancement is closely linked to the generation of EPR-type entanglement studied here [49], warranting further study.

The authors acknowledge productive discussions with C. Møller, R. A. Thomas, and A. Sørensen. This work was supported by the ERC AdG grant Quantum-N, the ARO Grant No. W911NF and by John Templeton Foundation. X. H. is supported partly by the China Scholarship Council (201606010044). E. Z. is supported by the Carlsberg Foundation. X. H. and Q. H. acknowledge the support of the National Key R&D Program of China (Grant No. 2016YFA0301302) and National Natural Science Foundation of China (Grants No. 11622428 and No. 61475006). D. V. acknowledges support of the Austrian Science Fund SFB FoQuS (FWF Project No. F4016-N23) and the European Research Council (ERC) Synergy Grant UQUAM. K. H. acknowledges support by Deutsche Forschungsgemeinschaft (DFG) through CRC 1227 (DQ-mat), project A05. X. H. is grateful to E. S. P. for hosting her during her stays at NBI.

*zeuthen@nbi.ku.dk

†qiongyihe@pku.edu.cn

- [1] R. Horodecki, P. Horodecki, M. Horodecki, and K. Horodecki, *Rev. Mod. Phys.* **81**, 865 (2009).
- [2] V. Giovannetti, S. Lloyd, and L. Maccone, *Science* **306**, 1330 (2004).
- [3] L. Pezzè, A. Smerzi, M. K. Oberthaler, R. Schmied, and P. Treutlein, *arXiv:1609.01609* [*Rev. Mod. Phys.* (to be published)].
- [4] I. D. Leroux, M. H. Schleier-Smith, and V. Vuletić, *Phys. Rev. Lett.* **104**, 250801 (2010).
- [5] O. Hosten, N. J. Engelsen, R. Krishnakumar, and M. A. Kasevich, *Nature (London)* **529**, 505 (2016).
- [6] R. J. Sewell, M. Koschorreck, M. Napolitano, B. Dubost, N. Behbood, and M. W. Mitchell, *Phys. Rev. Lett.* **109**, 253605 (2012).
- [7] W. Wasilewski, K. Jensen, H. Krauter, J. J. Renema, M. V. Balabas, and E. S. Polzik, *Phys. Rev. Lett.* **104**, 133601 (2010).
- [8] B. Julsgaard, A. Kozhekin, and E. S. Polzik, *Nature (London)* **413**, 400 (2001).
- [9] H. Krauter, C. A. Muschik, K. Jensen, W. Wasilewski, J. M. Petersen, J. I. Cirac, and E. S. Polzik, *Phys. Rev. Lett.* **107**, 080503 (2011).
- [10] K. C. Lee, M. R. Sprague, B. J. Sussman, J. Nunn, N. K. Langford, X.-M. Jin, T. Champion, P. Michelberger, K. F. Reim, D. England, D. Jaksch, and I. A. Walmsley, *Science* **334**, 1253 (2011).

- [11] R. Riedinger, A. Wallucks, I. Marinković, C. Löschnauer, M. Aspelmeyer, S. Hong, and S. Gröblacher, *Nature (London)* **556**, 473 (2018).
- [12] C. F. Ockeloen-Korppi, E. Damskägg, J.-M. Pirkkalainen, M. Asjad, A. A. Clerk, F. Massel, M. J. Woolley, and M. A. Sillanpää, *Nature (London)* **556**, 478 (2018).
- [13] G. Kurizki, P. Bertet, Y. Kubo, K. Mølmer, D. Petrosyan, P. Rabl, and J. Schmiedmayer, *Proc. Natl. Acad. Sci. U.S.A.* **112**, 3866 (2015).
- [14] M. Tsang and C. M. Caves, *Phys. Rev. X* **2**, 031016 (2012).
- [15] E. S. Polzik and K. Hammerer, *Ann. Phys. (Amsterdam)* **527**, A15 (2015).
- [16] K. Hammerer, A. S. Sørensen, and E. S. Polzik, *Rev. Mod. Phys.* **82**, 1041 (2010).
- [17] G. Vasilakis, H. Shen, K. Jensen, M. Balabas, D. Salart, B. Chen, and E. S. Polzik, *Nat. Phys.* **11**, 389 (2015).
- [18] W. Muessel, H. Strobel, D. Linnemann, D. B. Hume, and M. K. Oberthaler, *Phys. Rev. Lett.* **113**, 103004 (2014).
- [19] R. McConnell, H. Zhang, J. Hu, S. Cuk, and V. Vuletic, *Nature (London)* **519**, 439 (2015).
- [20] J. Kohler, J. A. Gerber, E. Dowd, and D. M. Stamper-Kurn, *Phys. Rev. Lett.* **120**, 013601 (2018).
- [21] E. Vetsch, D. Reitz, G. Sagué, R. Schmidt, S. T. Dawkins, and A. Rauschenbeutel, *Phys. Rev. Lett.* **104**, 203603 (2010).
- [22] J.-B. Béguin, E. M. Bookjans, S. L. Christensen, H. L. Sørensen, J. H. Müller, E. S. Polzik, and J. Appel, *Phys. Rev. Lett.* **113**, 263603 (2014).
- [23] C. Grezes, B. Julsgaard, Y. Kubo, M. Stern, T. Umeda, J. Isoya, H. Sumiya, H. Abe, S. Onoda, T. Ohshima, V. Jacques, J. Esteve, D. Vion, D. Esteve, K. Mølmer, and P. Bertet, *Phys. Rev. X* **4**, 021049 (2014).
- [24] P. Jobez, C. Laplane, N. Timoney, N. Gisin, A. Ferrier, P. Goldner, and M. Afzelius, *Phys. Rev. Lett.* **114**, 230502 (2015).
- [25] M. Gündoğan, P. M. Ledingham, K. Kutluer, M. Mazzer, and H. de Riedmatten, *Phys. Rev. Lett.* **114**, 230501 (2015).
- [26] A. Jöckel, A. Faber, T. Kampschulte, M. Korppi, M. T. Rakher, and P. Treutlein, *Nat. Nanotechnol.* **10**, 55 (2015).
- [27] N. Spethmann, J. Kohler, S. Schreppler, L. Buchmann, and D. M. Stamper-Kurn, *Nat. Phys.* **12**, 27 (2016).
- [28] K. A. Gilmore, J. G. Bohnet, B. C. Sawyer, J. W. Britton, and J. J. Bollinger, *Phys. Rev. Lett.* **118**, 263602 (2017).
- [29] J. D. Teufel, T. Donner, D. Li, J. W. Harlow, M. S. Allman, K. Cicak, A. J. Sirois, J. D. Whittaker, K. W. Lehnert, and R. W. Simmonds, *Nature (London)* **475**, 359 (2011).
- [30] R. W. Peterson, T. P. Purdy, N. S. Kampel, R. W. Andrews, P.-L. Yu, K. W. Lehnert, and C. A. Regal, *Phys. Rev. Lett.* **116**, 063601 (2016).
- [31] W. H. P. Nielsen, Y. Tsaturyan, C. B. Møller, E. S. Polzik, and A. Schliesser, *Proc. Natl. Acad. Sci. U.S.A.* **114**, 62 (2017).
- [32] C. F. Ockeloen-Korppi, E. Damskägg, J.-M. Pirkkalainen, A. A. Clerk, M. J. Woolley, and M. A. Sillanpää, *Phys. Rev. Lett.* **117**, 140401 (2016).
- [33] H. Tan, L. F. Buchmann, H. Seok, and G. Li, *Phys. Rev. A* **87**, 022318 (2013).
- [34] M. Tsang and C. M. Caves, *Phys. Rev. Lett.* **105**, 123601 (2010).
- [35] M. J. Woolley and A. A. Clerk, *Phys. Rev. A* **87**, 063846 (2013).
- [36] M. H. Wimmer, D. Steinmeyer, K. Hammerer, and M. Heurs, *Phys. Rev. A* **89**, 053836 (2014).
- [37] F. Bariani, H. Seok, S. Singh, M. Vengalattore, and P. Meystre, *Phys. Rev. A* **92**, 043817 (2015).
- [38] A. Motazedifard, F. Bemani, M. H. Naderi, R. Roknizadeh, and D. Vitali, *New J. Phys.* **18**, 073040 (2016).
- [39] C. B. Møller, R. A. Thomas, G. Vasilakis, E. Zeuthen, Y. Tsaturyan, M. Balabas, K. Jensen, A. Schliesser, K. Hammerer, and E. S. Polzik, *Nature (London)* **547**, 191 (2017).
- [40] C. A. Muschik, E. S. Polzik, and J. I. Cirac, *Phys. Rev. A* **83**, 052312 (2011).
- [41] D. V. Vasilyev, C. A. Muschik, and K. Hammerer, *Phys. Rev. A* **87**, 053820 (2013).
- [42] M. J. Woolley and A. A. Clerk, *Phys. Rev. A* **89**, 063805 (2014).
- [43] C. W. Gardiner, *Phys. Rev. Lett.* **70**, 2269 (1993).
- [44] C. Gardiner and P. Zoller, *Quantum Noise* (Springer-Verlag, Berlin, Heidelberg, 2004).
- [45] H. J. Carmichael, *Phys. Rev. Lett.* **70**, 2273 (1993).
- [46] R. Simon, *Phys. Rev. Lett.* **84**, 2726 (2000).
- [47] V. Giovannetti, S. Mancini, D. Vitali, and P. Tombesi, *Phys. Rev. A* **67**, 022320 (2003).
- [48] M. Aspelmeyer, T. J. Kippenberg, and F. Marquardt, *Rev. Mod. Phys.* **86**, 1391 (2014).
- [49] See Supplemental Material at <http://link.aps.org/supplemental/10.1103/PhysRevLett.121.103602> which includes Refs. [50–56], for details on the spin-optomechanical implementation, conditional stochastic master equation, steady-state entanglement optimization, and a comparison between unconditional entanglement and force sensitivity.
- [50] T. Holstein and H. Primakoff, *Phys. Rev.* **58**, 1098 (1940).
- [51] W. Wasilewski, T. Fernholz, K. Jensen, L. S. Madsen, H. Krauter, C. Muschik, and E. S. Polzik, *Opt. Express* **17**, 14444 (2009).
- [52] K. Stannigel, P. Rabl, and P. Zoller, *New J. Phys.* **14**, 063014 (2012).
- [53] V. P. Belavkin, *Commun. Math. Phys.* **146**, 611 (1992).
- [54] O. Černotík, D. V. Vasilyev, and K. Hammerer, *Phys. Rev. A* **92**, 012124 (2015).
- [55] A. A. Clerk, M. H. Devoret, S. M. Girvin, F. Marquardt, and R. J. Schoelkopf, *Rev. Mod. Phys.* **82**, 1155 (2010).
- [56] G. Turin, *IRE Trans. Inf. Theory* **6**, 311 (1960).
- [57] K. Hammerer, M. Aspelmeyer, E. S. Polzik, and P. Zoller, *Phys. Rev. Lett.* **102**, 020501 (2009).
- [58] J. T. Barreiro, M. Müller, P. Schindler, D. Nigg, T. Monz, M. Chwalla, M. Hennrich, C. F. Roos, P. Zoller, and R. Blatt, *Nature (London)* **470**, 486 (2011).
- [59] H. M. Wiseman and G. J. Milburn, *Quantum Measurement and Control* (Cambridge University Press, Cambridge, England, 2010).
- [60] Q. He, L. Rosales-Zarate, G. Adesso, and M. D. Reid, *Phys. Rev. Lett.* **115**, 180502 (2015).
- [61] N. Walk, S. Hosseini, J. Geng, O. Thearle, J. Y. Haw, S. Armstrong, S. M. Assad, J. Janousek, T. C. Ralph, T. Symul, H. M. Wiseman, and P. K. Lam, *Optica* **3**, 634 (2016).
- [62] E. Zeuthen *et al.* (to be published).